2017

USING LiDAR TO MAP THE GEOLOGY AND MORPHOLOGY OF ALLUVIAL FANS: SALTON SEA AREA, CALIFORNIA

Eric Alexander Macleod
Michigan Technological University, eamacleo@mtu.edu

USING LiDAR TO MAP THE GEOLOGY AND MORPHOLOGY OF ALLUVIAL FANS: SALTON SEA AREA, CALIFORNIA

By

Eric Alexander MacLeod

A REPORT

Submitted in partial fulfillment of the requirements for the degree of

MASTER OF SCIENCE

In Geology

MICHIGAN TECHNOLOGICAL UNIVERSITY

2017

This report has been approved in partial fulfillment of the requirements for the Degree of MASTER OF SCIENCE in Geology.

Department of Geological Mining and Engineering Sciences

Report Advisor:	*James R. Wood*
Committee Member:	*Ann Maclean*
Committee Member:	*Alexandria Guth*
Department Chair:	*John S. Gierke*

Dedication

To my Father and Family, who believed in and supported me through my academic endeavors.

Thank you

Table of Contents

List of Figures

List of Tables

Acknowledgements

I would like to thank my advisor Dr. James Wood, for his support and advice through my Master's program. This report would not have been also possible without the support and contributions from my committee members: Dr, Ann Maclean and Dr. Alexandria Guth. I would also like to thank Dr, John Gierke, for his support and advice he gave through my Peace Corps service and for his help when I returned. The Graduate School's office Dr. Nancy Byers Sprague for all the support and logistics; as well as The Department of Geological & Mining Engineering & Science (GMES) Staff: Amie Ledgerwood, Kelly McLean and Brittany Buschell for their assistance. All these individuals were very patient with me, and give me the encouragement and advise to help me complete this report. Attending Michigan Technology University as part of the Peace Corp Master's International program was not only an international adventure but an intellectual journey.

Thank you

Abstract

The main result of this study has been to show that detailed maps of the geology and morphology of alluvial fans can be generated from high spatial resolution (1-meter) DEM's (Digital Elevation Models) obtained from LiDAR (Light Detection and Ranging) data. DEMs with spatial resolutions of 1-meter, 10-meters and 30-meters were all examined but it was determined that only the 1-meter LiDAR data had sufficient spatial resolution to produce satisfactory maps of the geology and morphology. A case study on an alluvial fan in the Santa Rosa mountains northeast of the Salton Sea (California) showed that 1-meter spatial resolution LiDAR data could be used by itself to generate a detailed map of an alluvial fan that not only delineated the fan but also permitted detection and accurate mapping of various components of the fan such as debris flows, channel flows and sheet flows. The maps also revealed unique signatures for recent beach shorelines and showed features that were interpreted as levees in an active channel that ran through the alluvial fan. Profiles across the fan revealed the expected concave and convex morphology. These features were detected in sufficient detail to deduce an unambiguous geologic history as well as regions where the various processes interacted.

In addition to the geology/morphology maps, a statistical analysis comparing the 1-meter, 10-meter and 30-meter DEMs using the Spearmen Rank Correlation and Pearson Correlation showed no difference among the images. This suggests that elevation range is not influencing the images but rather it is the geospatial resolution that determines the details of the DEM and the Quaternary geological map.

Keywords: DEM's (Digital Elevation Models), LiDAR (Light Detection and Ranging), Quaternary geological maps, Alluvial Fans, Salton Sea

Introduction

The derivation of geologic information from digital topographic datasets is an important tool for studying geomorphological processes. Technological advances in storing and analyzing topographic information in a Geographic Information System (GIS) environment is extremely useful for mitigating potential geological hazards in areas of expanding urbanization. Digital Elevation Models (DEMs) provide a numerical representation of topography and is composed of equal-sized grid cells or pixels storing elevation information (Chang, 2016). DEM are usually interpolated to establish different elevation values for an entire terrain which is an array representation of pixels with an elevation value associated to each pixel as a function of geographic location (Tian-Xiang 2007; Arun P.V. 2013). DEMs can be obtained from contour lines in topographic maps, field surveys, photogrammetry techniques, radar interferometry (i.e. Interferometric synthetic aperture radar (InSAR)), and imaging laser altimetry (Manuel, 2004; Dong, 2014). The resolution of the DEMs is dependent on the technology which determines the spatial resolution (i.e. 30-meter, 10-meter or 1-meter) of the image.

ArcMap 10.4 was the main software product for this report. Recognizing spatial patterns based on elevation change is an important use of DEMs. A comprehensive suite of tools has been developed to analyze DEMs to determine: slope, curvature, aspect, texture, contour shape and drainage pattern and associated geomorphologic features (i.e. alluvial fans, aeolian deposits, rivers). It is imperative for engineers and scientists to understand sediment transportation and the deposition of alluvial sediments along active

flood regions. Part of understanding Earth surface features is to produce better geological maps which are needed to mitigate geologic hazards (e.g. flooding and debris flows), for studying the complex interplay between endogenous dynamics (e.g. tectonics) and exogenous processes (e.g. erosion and alluvial deposits) that have occurred throughout Earth evolution and how urbanization is affected by the aforementioned (Gianluca et al.,, 2016).

Map making is one of the oldest trades that still has an economical demand in society where it is an integral science. The display and design of a map draws attention to areas that the cartographer wants the user to observe. The need to produce accurate maps that emphasize a particular interest of study has become more refined in recent years. For example, in California Governor Arnold Schwarzenegger established in 2003 the Alluvial Fan Task Force (AFTF) for an in-depth study of how alluvial fans contribute to flood hazards (Benrossian, T.L, 2014). Maps focusing on Quaternary deposits, need to identify the fine details for an accurate Quaternary geological map. The accuracy of DEMs and associated interpolation techniques have been conducted and the results are not consistent (Chen,2013).

Objective

The focus of this study is to evaluate the utility of 1-meter DEM generated from Light Detection and Ranging (LiDAR) and compare it to 10 and 30-meter DEM typically generated by photogrammetric methods from stereo imagery (Mukherjeea Sandip., 2012).

Regardless of spatial resolution DEM approximates a real-world continuous elevation surface (Tian-Xiang Yue 2007). The purpose of this study was twofold. First, we aimed to construct a geovisualization using different spatial resolution from the DEMs to create topographic map overlay on top of a hillshade model to give it a 3-dimensional effect. Using different contour intervals of 10, 5 and 1-meter to observe if the topographic map preserves the geomorphological features we then developed a detailed Quaternary geological map of the alluvial fans in the study area. The second objective is in the appendix section, we determined if the information controlled by the DEMs differs between spatial resolution using a nonparametric statistical method. By evaluating the correlation between the 10-meter and 30-meter DEMs to the 1-meter DEM, we determined if the spatial resolution impacts the information content of the DEM. This was done by using Pearson and Spearmen's Rank Correlations (see appendix A and appendix B).

Study Site

The study is located in the northwest region of the Salton Sea. An unincorporated area that borders the northwest corner of Imperial County, California (Figure 1). The study area is the Torres Martinez Indian Reservation that encompasses the town of Salton Sea Beach, and highway 86; it is geographically situated near the Santa Rosa Mountains just north of Rainbow Rock where the terrain is rugged with steep slopes. The alluvial fan, ancient shorelines and flood plains make it an ideal location to compare different spatial resolution of DEMs for Quaternary deposition delineation and mapping.

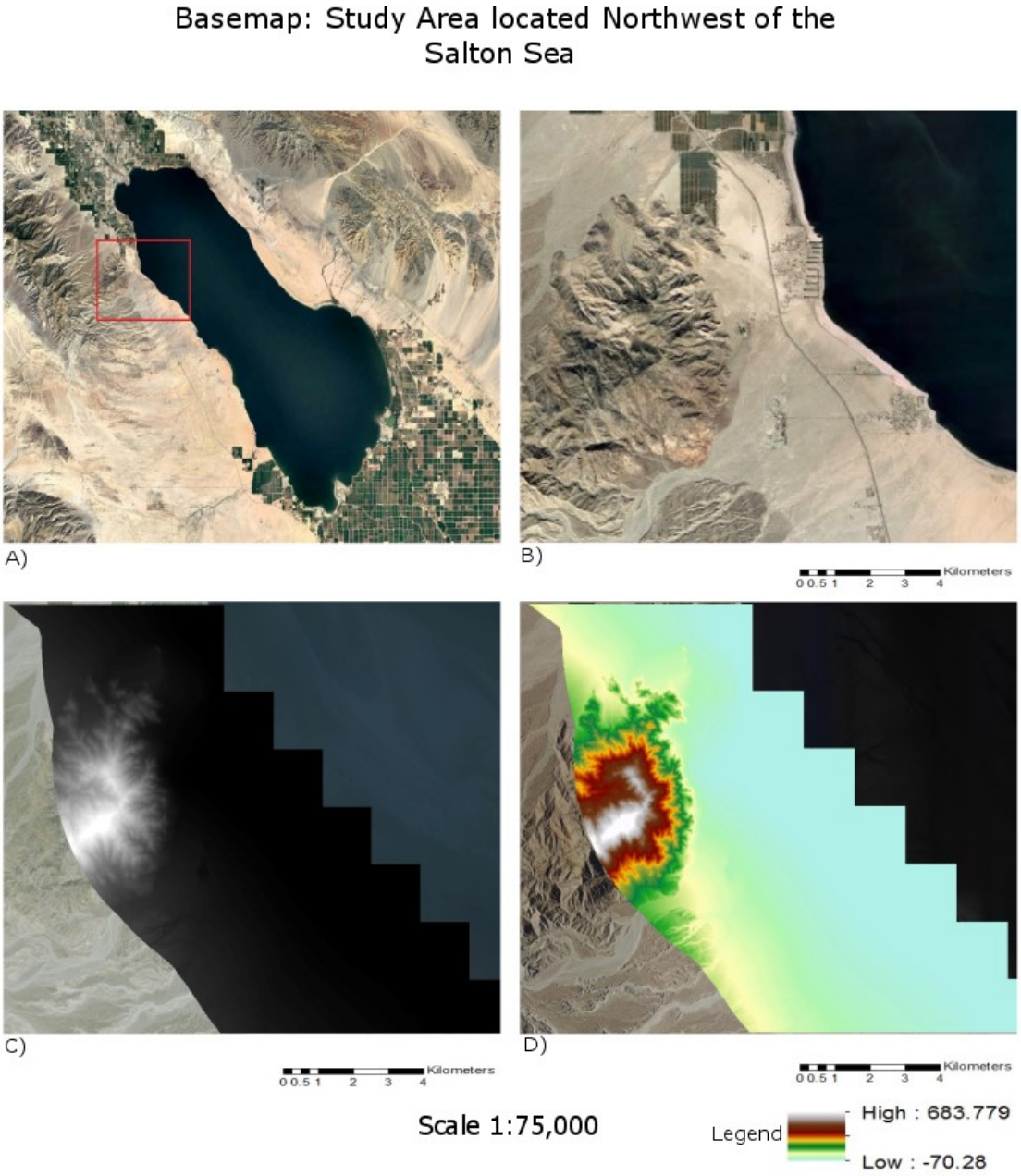

Figure 1. The area of study is located northwest of the Salton Sea at the junction of Imperial County, San Diego County and Riverside county. A) An over-view if the Salton Sea and the box in red is the study area. B) Closer look at the area of study. C and D) Digital elevation model (DEM) are one of the same and overlaid on top of the outcrop. The black and white image is the robust DEM with no changes; the other image was inhance using ArcMap to show a clear distinction of the elevation.

Images are provided by Google Earth and National View at USGS.

Regional Geology

The Salton Sea, often referred to as the Salton Trough is a transtensional (dextral) region drifting from the North American Plate (NAP) and forming the present-day basin (Ingersoll, 2008). The northwestern section of the Salton Sea region consists of bajada landforms that coalesces several alluvial fans, that appear to have been eroded by rising levels of the Salton Sea. The regional geology is structurally complex, bounded by faults, basement uplifts and sedimentary deposition towards the Salton Trough. These processes took formation approximately during the late Cenozoic rifting and transtensional strain events which occurred proximal to the present-day location of the San Andreas fault (Dibblee, 1954; Woodard,1963; Winker, 1987; Winker and Kidwell, 1996; Lutz, A.T., 2006).

While there is no in-depth study of the location area to reference, only the maps of Dibble (1954) and a paper on the stratigraphy by Lutz, A.T. (2006); illustrates the regional geology surrounding the study area. Lutz (2006) points out that the rock type is of Paleozoic metsedimentary and Mesozoic plutonic rock that is referred to as the Ocotillo formation. This formation is a part of the Santa Rosa Mountain range that has been influence by the San Felipe Hill (SFH), Santa Rosa fault (SRF) and the West Salton detachment fault (WSDF). The WSDF system is the result of a supradetachment basin; perhaps as recent as 1.1 Ma (Axen and Fletcher, 1998; Kirby, 2005; Steely et al., 2005; Dorsey, 2006; Steely, 2006). Lutz (2006) again pointed out that the formation cuts through the crystalline basement which comprises metasedimentary rocks, tonalite, granodiorite and mylonite created during the Cretaceous period (72 -145 Ma). The region is very seismically active

with the San Jacinto fault and other faults contributing to the orogenic processes of the Santa Rosa Mountains. The area of study is undergoing continuous mountain building and the fluctuation of the Salton Sea suggest that the alluvial fans deposition occurs at a slower rate. This gives the lithostratigraphic classification of a retrogradational formation of the alluvial fans (Boggs, 2006; Ingersoll, 2008).

Background of Alluvial Fans

Alluvial fans form when mountains experience erosional process during meteorological events. These landforms are formed by the aggradation of alluvial sediments, downslope from the emergence of channels, rivers, streams from a mountainous drainage basin (Harvey et al., 2005). Several studies have been devoted to analyzing the morphology and internal structure of alluvial fans, especially in regions located in arid and semiarid environments (Boggs, 2006). Alluvial fan development requires certain conditions in a geological setting which includes: (1) a topographic setting wherein the contributing channel the water collects onto the embankments of steep inclines and are confined to a single passageway that drains to a relatively flat open lowland adjoined to a valley, basin, or flood plain; (2) a plethora source of sediments coming from the mountainous catchment; (3) the area of discharge transports sediments from the drainage area to the fan; and (4) topographic features changes to a low-gradient conditions where the sediments accumulate. This builds the fan-shaped patterns of an alluvial fan. (Bull, 1977; Schick and Lekach, 1987; Webb et al., 1987; Blair and McPherson, 2009; Harvey, 2003; Mather et al., 2000; Florsheim, 2004; Gianluca, 2016).

The channel flows that cause flash-flooding and debris flows in arid and semi-arid regions occur in the southwestern United States are natural episodic flows and the dynamics of sediment transport can change the characteristics of a landscape during one flooding event. That is why it is imperative to understand the nature of alluvial fans so that accurate Quaternary Geological maps can be produced to help urban planners develop safe protocols when a flood event occurs.

Preferential treatment has been given towards perennial river systems for research and development purposes because the concepts and tools are easier to work with when there is a constant water supply; and in regions that are episodic can be problematic. Ephemeral systems and intermittent streams have been classified as “degraded” and their habitats undervalued (Stein at el, 2010). Understanding the episodic nature of the stream flows, floods and the dynamics of sediment transport can help mitigate floods (Miller, 2011).

Alluvial fan flooding was first brought to the attention of the federal government following catastrophic debris flows on alluvial fans near Rancho Mirage, California in September 1976 and July 1979 (Zhao, 1993; Raymond, 2010). The natural geological hazard showed that alluvial fan flooding had different characteristics than flooding in rivers. Hence requiring different maps and mitigation methodologies. When the Federal Emergency Management Agency (FEMA) was established in 1979 signed by President Carter Executive Order 12148 it assumed disaster relief efforts. This started the recognition of the uncertainty of alluvial fan flooding that needed to be addressed throughout the United States (FEMA, 2003).

California has its alluvial fan flooding planning efforts compiled by the United State Geological Survey (USGS). However, in 2003 Governor Arnold Schwarzenegger establish the Alluvial Fan Task Force (AFTF) and gave the responsibility to the Department of Conservation, and the California Geological Survey (DOC/CGS), with funding from the Department of Water Resources (DWR). Since that time, the AFTF has mapped a geologic compilation of quaternary surficial deposits in 10 counties shown in Figure 2 (San Bernardino, Riverside, Los Angeles, Ventura, Santa Barbara, San Luis Obispo, Kern, Orange, Imperial and San Diego counties), for identification and mapping of alluvial fan flood hazards (Trinda, 2010).

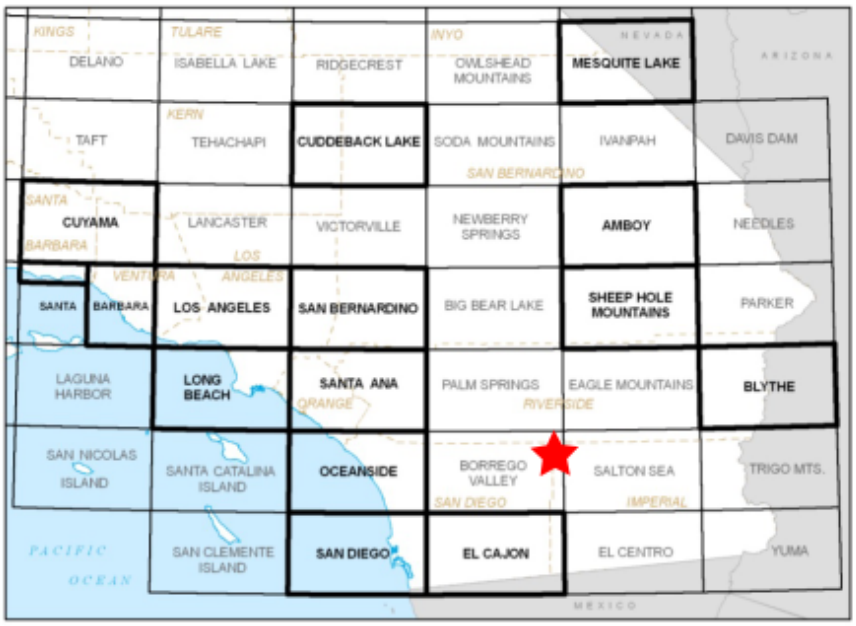

Figure 2: The red star is the study location. This map shows the Quadrangles of the area that the AFTF have mapped. The mapped areas are in bold taken from the Geologic Compilation of Quaternary Surficial Deposits in Southern California report (2010)

Spatial Resolution on Mapping Landforms

Spatial technology has allowed geologists, geographers and cartographers to map landforms indirectly to access areas that may be inaccessible. It has enabled scientists to observe characteristics of an outcrop that may not be easily seen by field geologist, especially when the landform is too large to be properly identified from the ground. Before the advancement of spatial technology, elevation data was typically represented as contour lines. Aerial and satellite imagery provide diverse array of spatial data. This study analyzed DEMs with spatial resolution of 1, 10 and 30-meters resolution. Images likes these provide information for measuring, mapping and monitoring Earth features.

Lower spatial resolution DEMs (i.e. 90 and 60-meters), were the first generation of DEMs. It wasn't until the technological advancement of higher resolution imagery, that 30- meter and 10-meter DEM's became available in the United States of America. The 30-meters DEM covers all United States and only selected regions have higher DEM spatial resolution (i.e. 1-meter LiDAR covers the coastal areas in the United States collected by NOAA). With the technological advancement, 90 and 60 – meter DEM have been phase out except for Alaska (USGS (a)). The 10-meter DEMs will eventually phase out the 30-meter DEM. Even higher spatial resolution LiDAR derived DEM such as 1-meter was acquired in 2010 by USGS only around the rim of the Salton Sea (CA). The dataset is an orthometric vertical datum NAVD88 using GEOID12A, was collected with light detection and ranging (LiDAR), and serviced by the OpenTopography website (USGS, 2010).

The ancillary data and other existing inventories used for this report were obtained from the United States Geological Survey (USGS) National Map website. The National Elevation Dataset (NED) provides the elevation layer for the National Map (USGS, 2016 a, b). Data from the National Elevation Dataset (NED) include 1 arc-second (30-meter), and 1/3 arc-second (10-meters) spatial resolutions. The 10-meter and 30-meter DEMs were derived independently.

Methods

To measure the accuracy of the Digital Elevation Models (DEMs) that have different cell sizes; an area in the study was specifically selected that shows an alluvial fan located near Salton Sea and the area surrounding Salton Sea Beach. Observing the Landsat images of the site, it shows active channels where braided streams traverse the landscape and the alluvial fan has a distinct signature or fingerprint of geomorphological features (Figure 3a and Figure 4). Along with the alluvial fan, ancient shorelines, flood plains additionally the site has low amount of vegetation so that the topographic detection will not be impaired. This study involves an interpolation technique that uses a geostatistical approach that is commonly employed in geomorphological research (Mitas and Mitasova, 1999). Techniques include comparing a linear regression relation between the different DEM using Pearson and Spearmen's Rank Correlation to see if the DEM are similar to each image base on elevation data that can be seen in appendix A. With the investigation, the implications of the findings were used to develop three topographic maps at an interval of 1-meter with ArcGIS derived from 30, 10 and 1-meter DEMs. This determined which

DEM is more accurate in selecting detailed information of the terrain by seen how the contours emphasize the geomorphology. As well as identifying details on human activities and alteration of the landscape with limited artifacts in the topographic map. The topographic map which produces the best quality image will be used as the basis of a new Quaternary geological map of the northwest Salton Sea alluvial fan near Salton Sea Beach.

Aerial View of Site with Radial and North-South Terrain Profiles

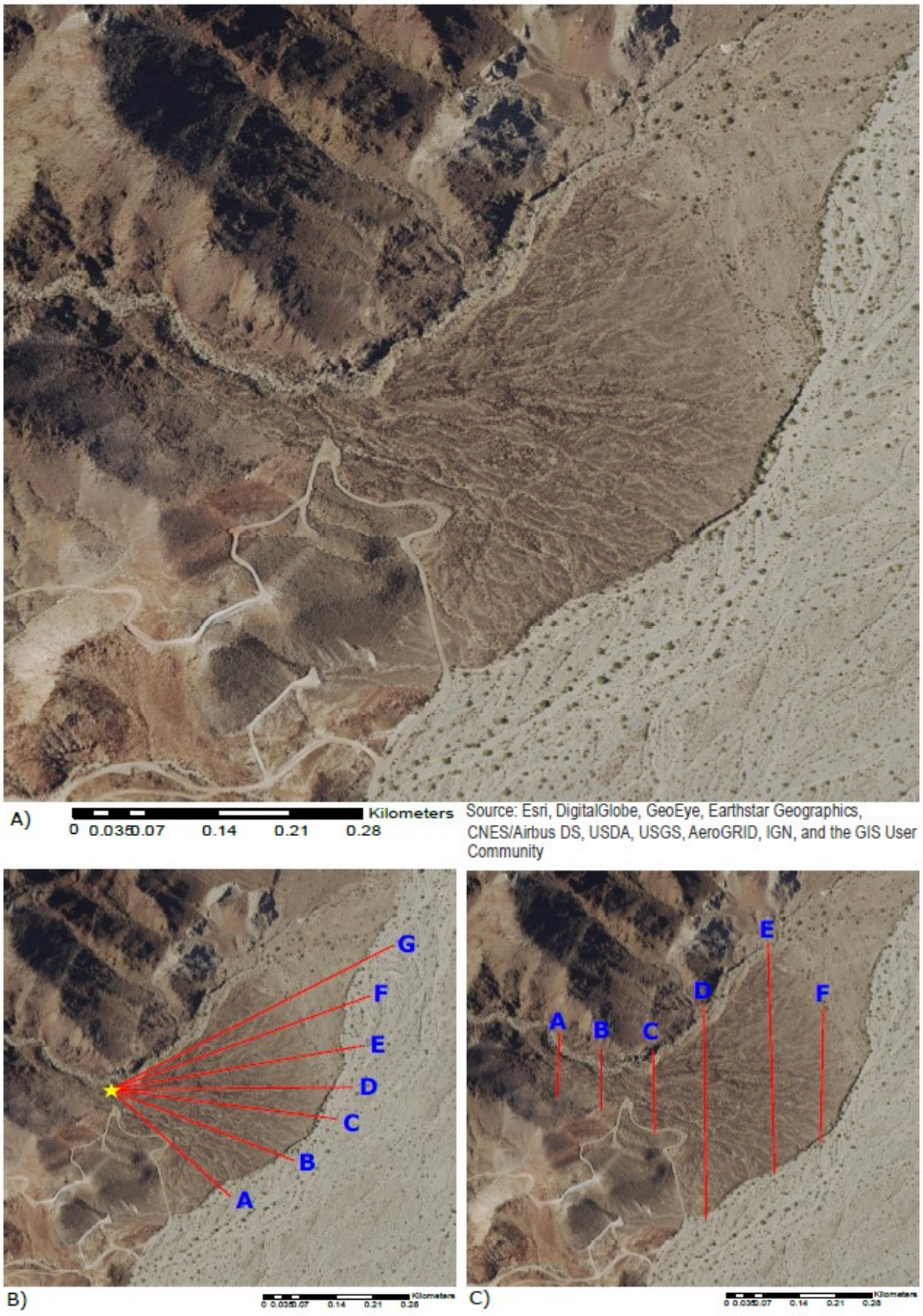

Figure 3. (A) An aerial view of the area of study, you can see where the active and inactive areas of the alluvial fan and the channel cut though the fan. (B) The red lines are cross-section running in a radial direction from the fan and the yellow star is starting point of these cross-sections. (C) The cross-sections run from the north-south direction starting from the mouth of the alluvial fan.

Data Preparation

The National Elevation Dataset and National Oceanic and Atmospheric Administration (NOAA), U.S. Department of Commerce provided the necessary imagery for this study. The National Elevation Dataset covers the whole United States with spatial resolutions from 10-meter to 30-meter DEM datasets and NOAA provided the high spatial resolution LiDAR dataset of 1-meter DEM of the whole coastal United States. Two different shapefiles were produced from each of the three DEMs. One shapefile corresponds to the digitized contour lines of the three DEM's, overlaid on a hillshade model with 50% transparence to enhance the image. Another shapefile is associated with the channels, and streams that cut through the alluvial fan were also used to interpret the geomorphology and quality of the DEMs.

Topographic Characterization

Before the advancement of satellite technology and image processing, a field geologist would design their geological maps using topographical maps. Topographical maps are still used in creating geological maps but the purpose of this study is to examine the different DEM spatial resolutions to see which DEM best illustrates terrain features since the elevation precision differs for each DEM. This can be done by creating three topographic maps and provides a clear geovisualization of the area of study. All in effort to allude towards a detail Quaternary Geological map of the alluvial fan in the northwest section of the Seaton Sea.

The details of the terrain features where done by creating topographic (topo) maps from each DEM using ArcGIS, with a contour interval of 1-meter. The necessary steps that are need are shown in Flow chart 1 to create contours lines for the topo map. It also shows the overall process of a watershed analysis for a more thorough investigation, however, the focus of this report is to create a detail topo map.

Flow chart 1

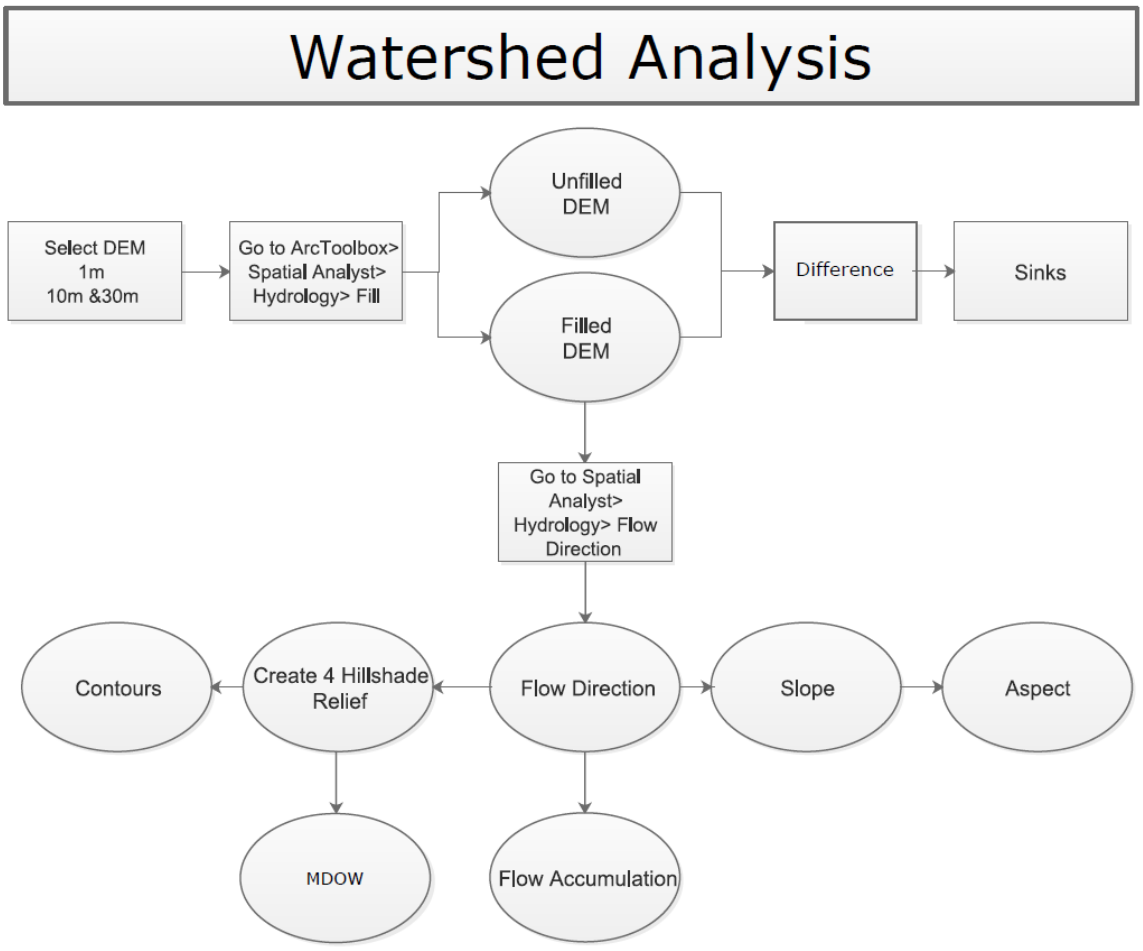

Before creating the topo map, all the DEMs had to be processed because the DEM data is not continuous, meaning there are sinks or voids in the DEMs that need to be filled. These voids ("sinks") are points in the DEM image that contain errors that need to be corrected. Saad, Shaker A (2015) mentions that the void occurs in two ways:

1. The cells that contains zero has the value appear when the outcrop is mountainous.
2. The cells contain noise where the landscape is flat.

The most common place for voids ("sinks") to occur noted by Davis Jenkins (2006) are in stream channels. When observing the location of these voids with a landsat image (Figure 1); we can see that the voids are in areas where the elevation changes drastically (i.e. channels, mountain cliffs). These voids need to be filled so that the illustrations (shown in flow chart 1); i.e. flow direction, hillshade, and other calculations; can be calculated correctly. Otherwise the ArcGIS algorithms will improperly output the illustrations. The 1-meter DEM has 83,748 voids, the 10-meter DEM has 2,079 voids and the 30-meter data has 167 voids. The size if the voids are the dimensions of the specified DEM cell (i.e. 1 meter, 10 meter), by filling the voids in the DEM data makes the image continuous.

The 1-meter DEM image was taken from LiDAR (Light Detection and Ranging) which is widely used to measure terrain features and producing topographic maps. Logically a 1-meter DEM should have more spatial data than DEMs with lower spatial resolution. ArcGIS provides the dimensions of the 1- meter DEM and we can see there are 16,395 columns, and 11,130 rows of spatial data. The high resolution would make is easier to characterize the geological features with great accuracy. The 10-meter DEM has 1246

columns, 1179 rows compared to the 30-meter DEM 392 columns, 371. This means that the density of data is decrease as the cell size increase, there is less spatial resolution and detail when using 1-meter DEM verse the 10 and 30-meter DEM.

Referring to flow chart 1, after filling in the voids (sinks) a topographic map of all three DEMs can be created. The area of figure 4 shows the region where the topo maps were created. The quarry, highway 86, Salton Sea Beach and drain channels are highlighted to emphasize the amount of detail the topo map produces in this area since there are natural and manmade structures. The topographic map of figure 5 shows clear features of the terrain slope, channels that were not able to be seen from figure 4 where the anthropogenic structures such as the quarry and Salton Sea Beach are clearly define in both figures. Feeder transport water to main active channels can be observed, mark as red dash lines in Figure 4, as well as the ancient shoreline (Figure 5) of the Salton Sea located just north of Salton Sea Beach. The contours that lie close to the Salton Sea are evenly space out, which indicates a smooth surface and gentle slope. This would be accurate given the geological history of the Salton Sea where the levels have risen all the way to the Santa Rosa Mountains. The contours also show some topographic relief (changes within an area), where the quarry is well defined, however some contour lines are distorted due to the sudden change in elevation causing the contour lines to map artifacts. These artifacts are the cells sizes of the 1-meter DEM that are being mapped as topography. The channels are very distinctive but difficult to read because the area is too large and has too much detail to be able to make an appropriate observation.

HWY 86 and Salton Sea Beach

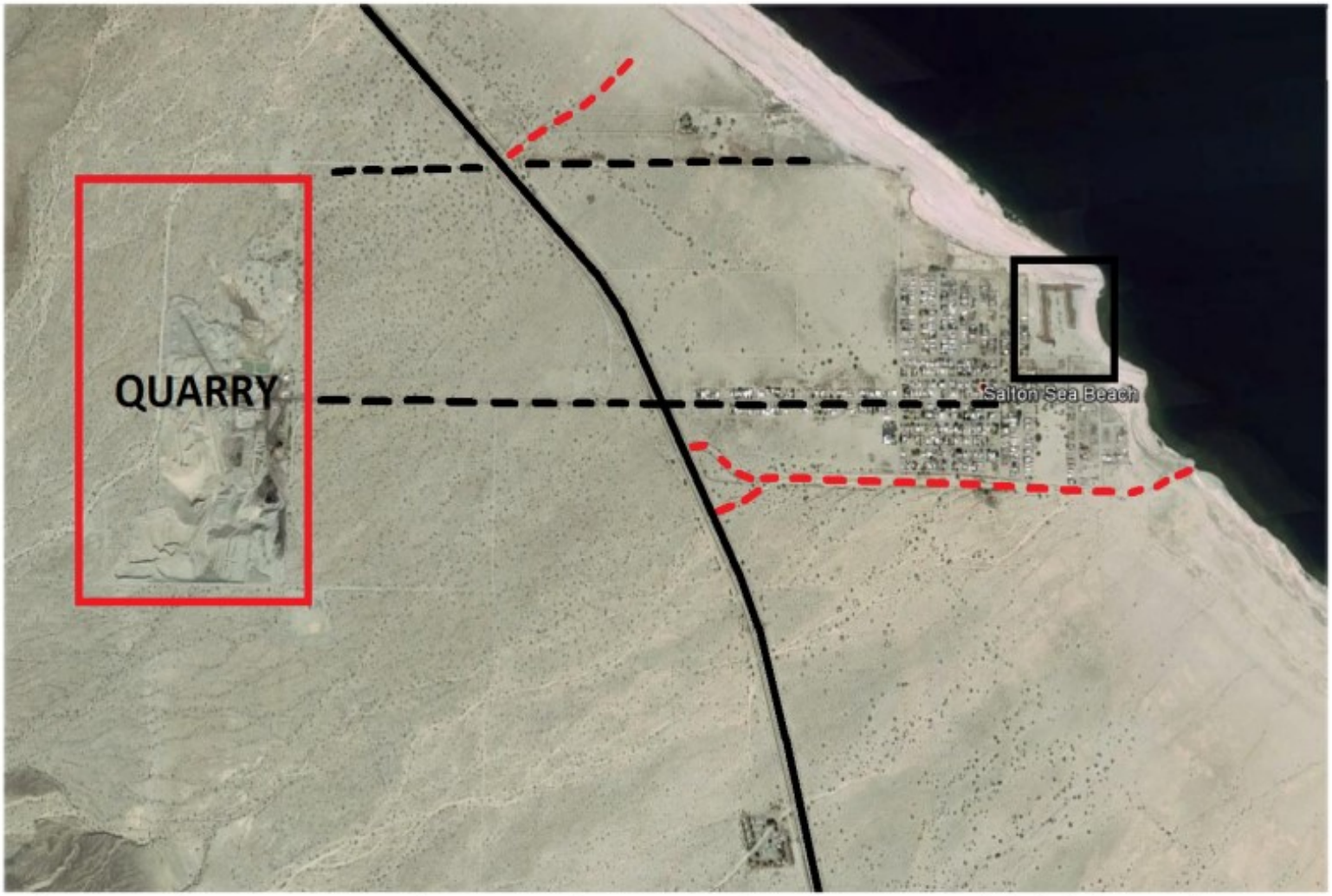

Figure 4: shows a quarry in the east, Salton Sea Beach in the west in the black box and HWY 86 running north to south between the two areas highlighted as a black line. The red dash lines are active channel and the black dash line are dirt roads.

Aerial View of Salton Sea Beach with 1m DEM with 1m CI

Figure 5. The contours are setup at 1 meter intervals, the 1 meter DEM with Hillshade model and Landsat image make the terrian easy obvere the channel flows towards the Salton Sea. The 1 meter DEM contours are able to output fine details of uban growth. HWY 86 is clearly define by the contours as well as the parking lot and dirt roads.

Figure 6 was produced with the 10-meter DEM where the cell size has increase 10 time as much as the 1-meter DEM and figure 7 is the 30-meter DEM and the cell size increase 30 times. These two images have the same contour interval as figure 5 (1-meter). It is immediately clear that the terrain appears smoother and less geological detail is visible as DEM spatial resolution decreases. As seen in figure 6 and figure 7, the anthropogenic structures are difficult to distinguish; such as highway 86 and the town of Salton Sea Beach. Even though figure 7 shows the orientation of the highway, the contours gave it an appearance of a geological anomaly rather than being obvious man-made features. Salton Sea Beach and the quarry contours lines produce artifacts within these anthropogenic structures and the structures make the map appear to have artifacts (digital errors). The ancient shoreline seems to stretch further towards the Santa Rosa Mountains and this is due to the smoothing of the terrain. The benefit of the lower resolution is that the large channel width is easier to discern. Taking away the finer details of the feeder channels to the main channel, the contour lines only pick up the main terrain features.

Based on the findings, and comparing it to the topographic maps that the USGS provides and to figure 6 and figure 7, it is advantageous to say figure 5 (1-meter DEM) shows the most details of the geological terrain and anthropogenic structures. This is because the topographic maps that were produced in this study are based on a probability density model which describes the distribution of data of the area (Bishop, 1998; Zheng Cui., 2013). Therefore, the quality of the topo map is based on the spatial distribution of the data that is provided by the DEM. Hence, the 1-meter DEM is better image to map the geomorphological features over the lower resolution.

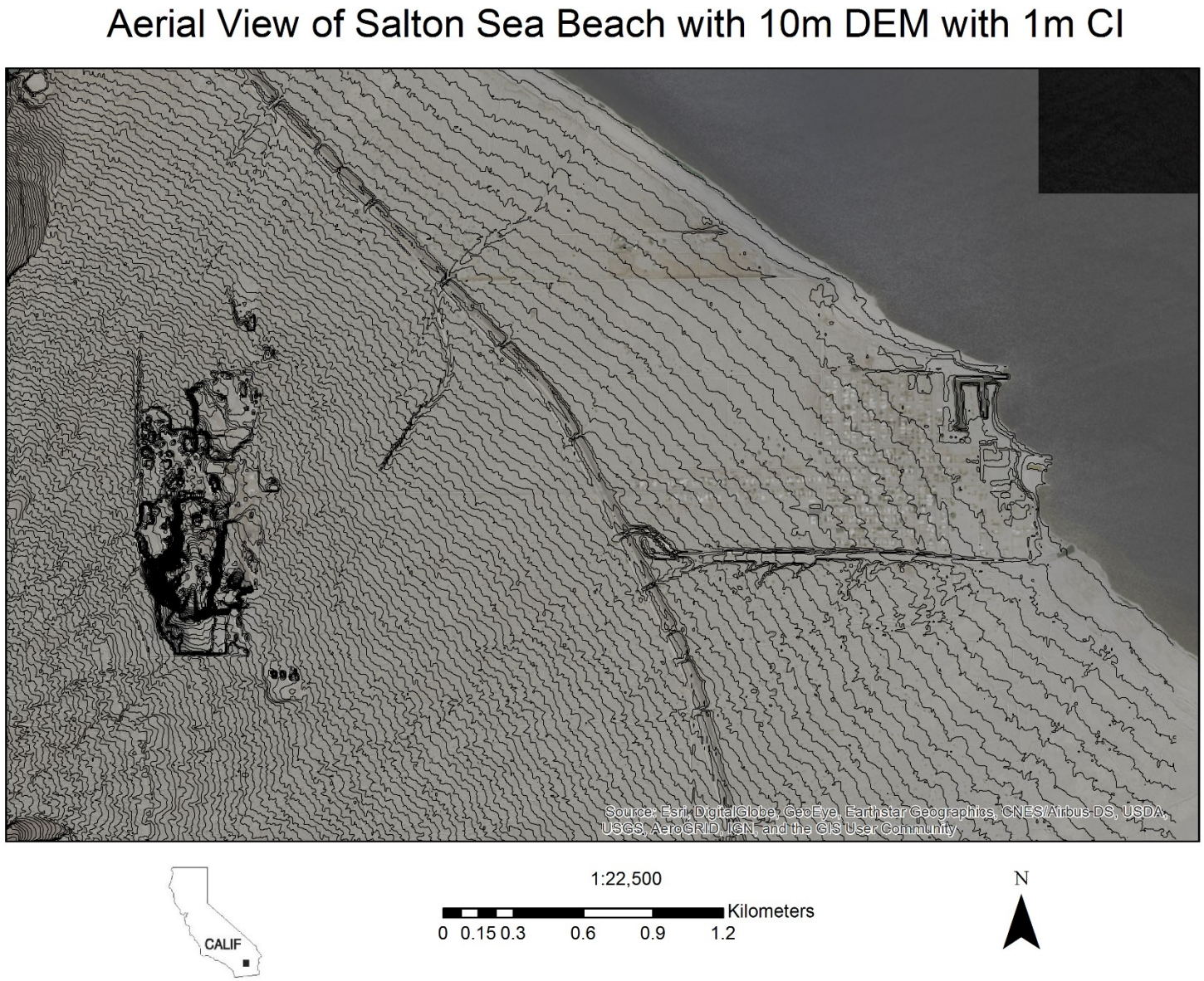

Figure 6. The anthropogenic structures are becoming difficult to distinguish and the contours are smoothing out.

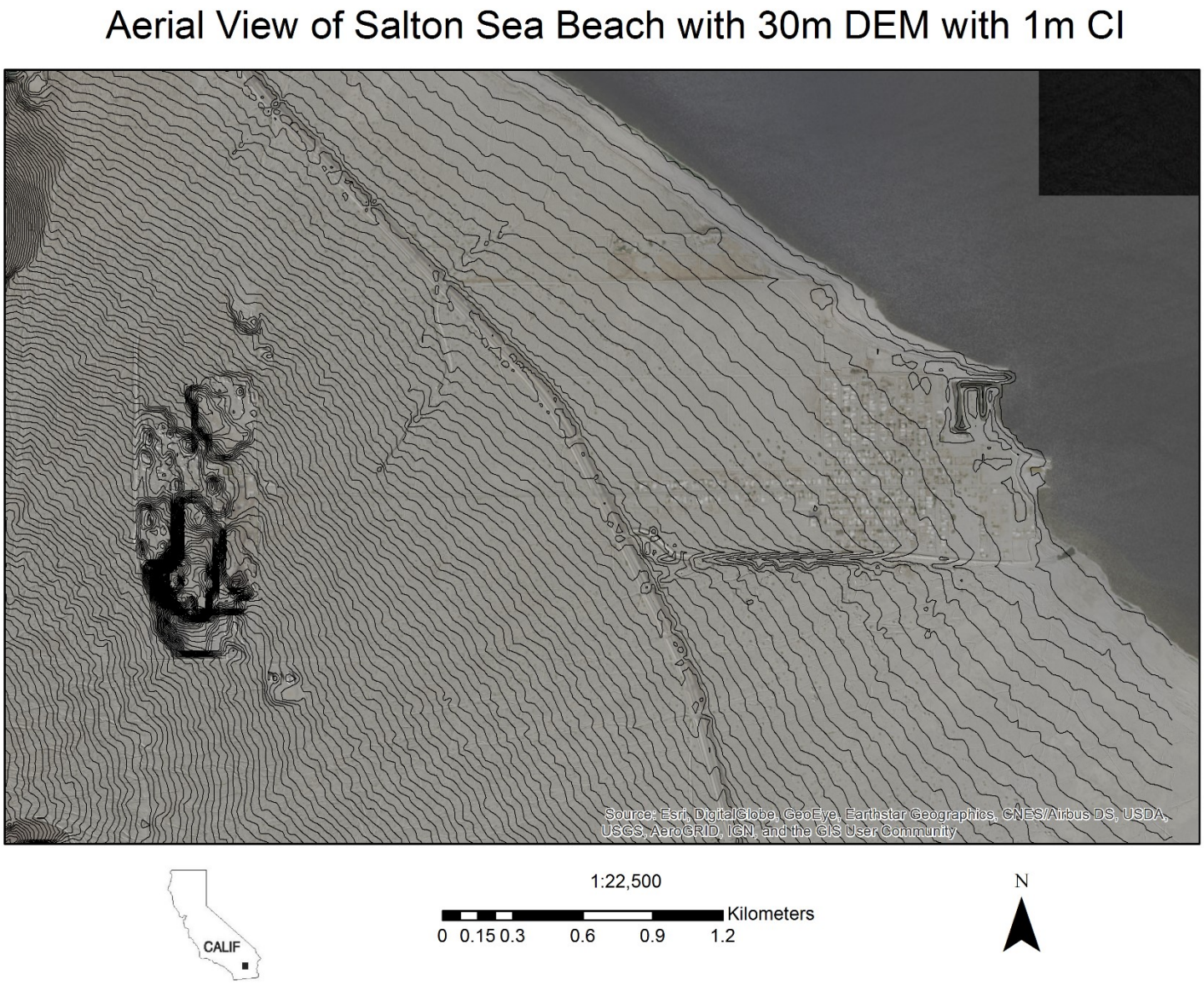

Figure 7. The 30-meter DEM and the pixels size is 30 times larger than the 1-meter DEM making the contours appear smoother and less detail of the terrain can be seen.

Digital Geological Mapping of the Alluvial Fan

Developing Quaternary geological map in flood prone areas, typically on alluvial fans was recognized by the National Research Council (NRC, 1996) and by FEMA as a priority in their 2003 guidebook. FEMA region IX gave the California Department of Water Resources the responsibility of monitoring and tracking alluvial fan hazards (FEMA, 2003). The California Department of Water Resources has an Alluvial Fan Task Force (AFTF) so that there would be more research on alluvial fans and how they contribute to flood hazards (Benrossian, T.L, 2014). They have mapped 10 counties in southern California, primarily in developed areas as seen in figure 2. However, there are no detailed maps on Quaternary deposits in unincorporated areas.

The unincorporated area of Salton Sea Beach, Imperial County, California; has no recent geological maps. The 1-meter DEM will be used to delineate the alluvial fan morphology that lies east of the quarry towards the Santa Rosa Mountains. The alluvial fan in figure 3 was chosen not only because of its proximity to Salt Sea Beach but because of the unique geomorphological features the topo map displays and the limited LiDAR data that is available. The topo map created using flow chart 2 in ArcMAP to trim the DEM to focus on the area of study. This topo map was created using 1-meter DEM seen in figure 9. The upper corer of the topo map, shows the same features that were observed in figure 5, figure 6 and figure 7, where the ancient shoreline of the Salton Sea once resided. Southwest of the topo map contours lines can be seen evenly spaced-out and directional flow of small channels shows evidence of flash flooding. The area is a flood plain or a sheet flow that has eroded the base of the alluvial fan. The alluvial fan is very distinctive

in the topo map where the active channel flows downstream through a laterally confined mountainous valley that cuts through the alluvial fan, and ancient shoreline then bleeds to a non-confined lowland of the flood plain.

Flow-Chart 2

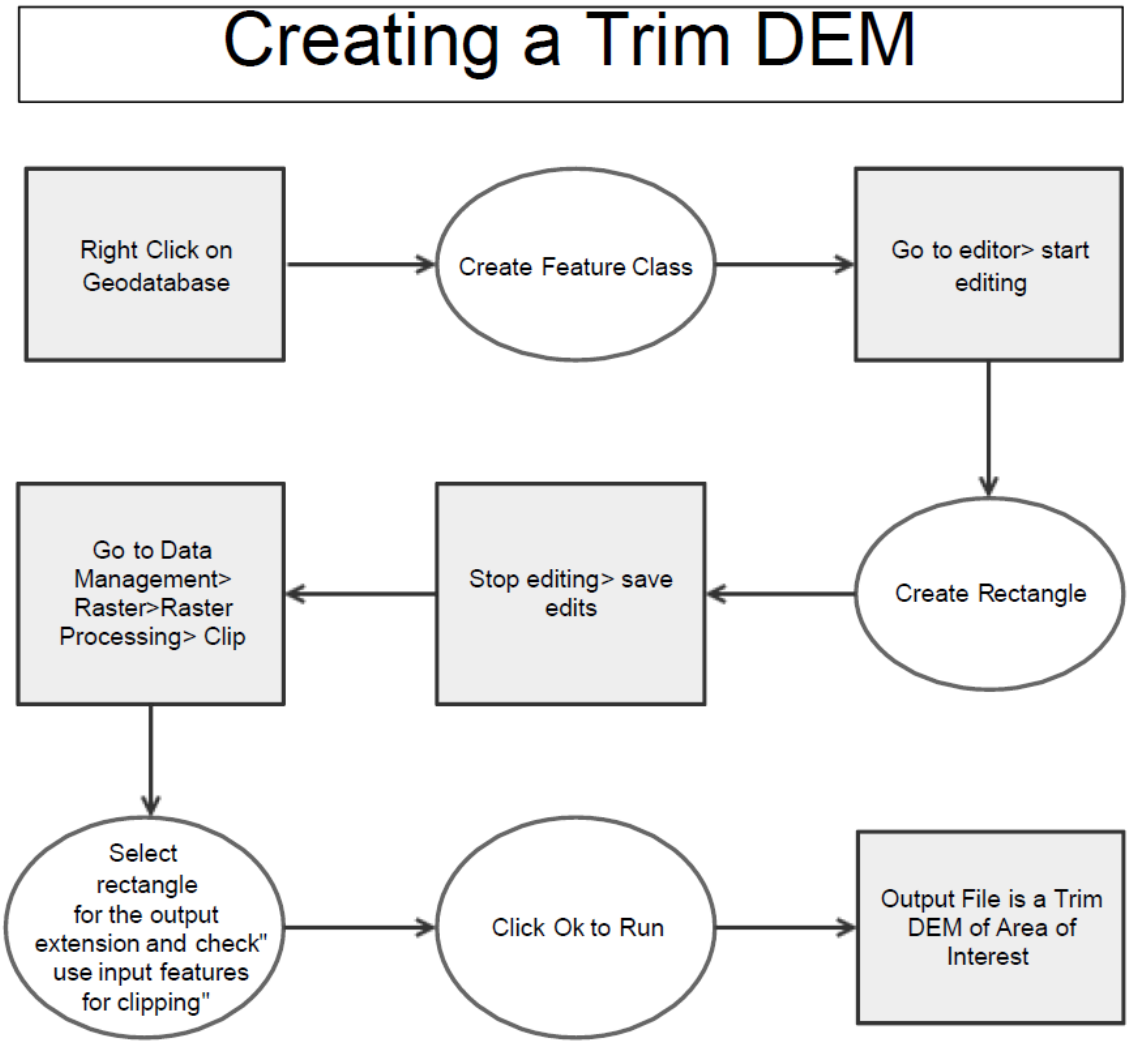

Characterizing the morphology of the alluvial fan with the 1-meter DEM will help to further delineate the evolution of the fan. Two profiles of the alluvial fan were analyzed by creating traces along the alluvial fan seen in figure 3b and figure 3c. The elevation of figure 3b and figure 3c were traced with ArcMAP and calculated using MatLab. The cross-sections of the alluvial fan show the curvature of the fan morphology. These traces align in the radial direction shown in figure 3b that corresponds to the profile of figure 9. Figure 3c alignment is in the north - south direction and corresponds to profile figure 10. Where the traces end, it marks the change of the slope profile of the fan. It is difficult to see but the cross-section from ‘a’ to ‘g’ starts out convex to concave retrospectivity. According to Stock J.D. (2008) this is related to how sediments are transported; longer profiles are commonly concave up and the shorter fans are generally convex. In contrast, the cross-sections of figure 9 show how the sediments are dispersed. There is higher density of material in profile A and has a slight convex morphology. Moving towards profile G a slight concave morphology can be observed.

Aerial View of Study area with 1m DEM with 1m CI

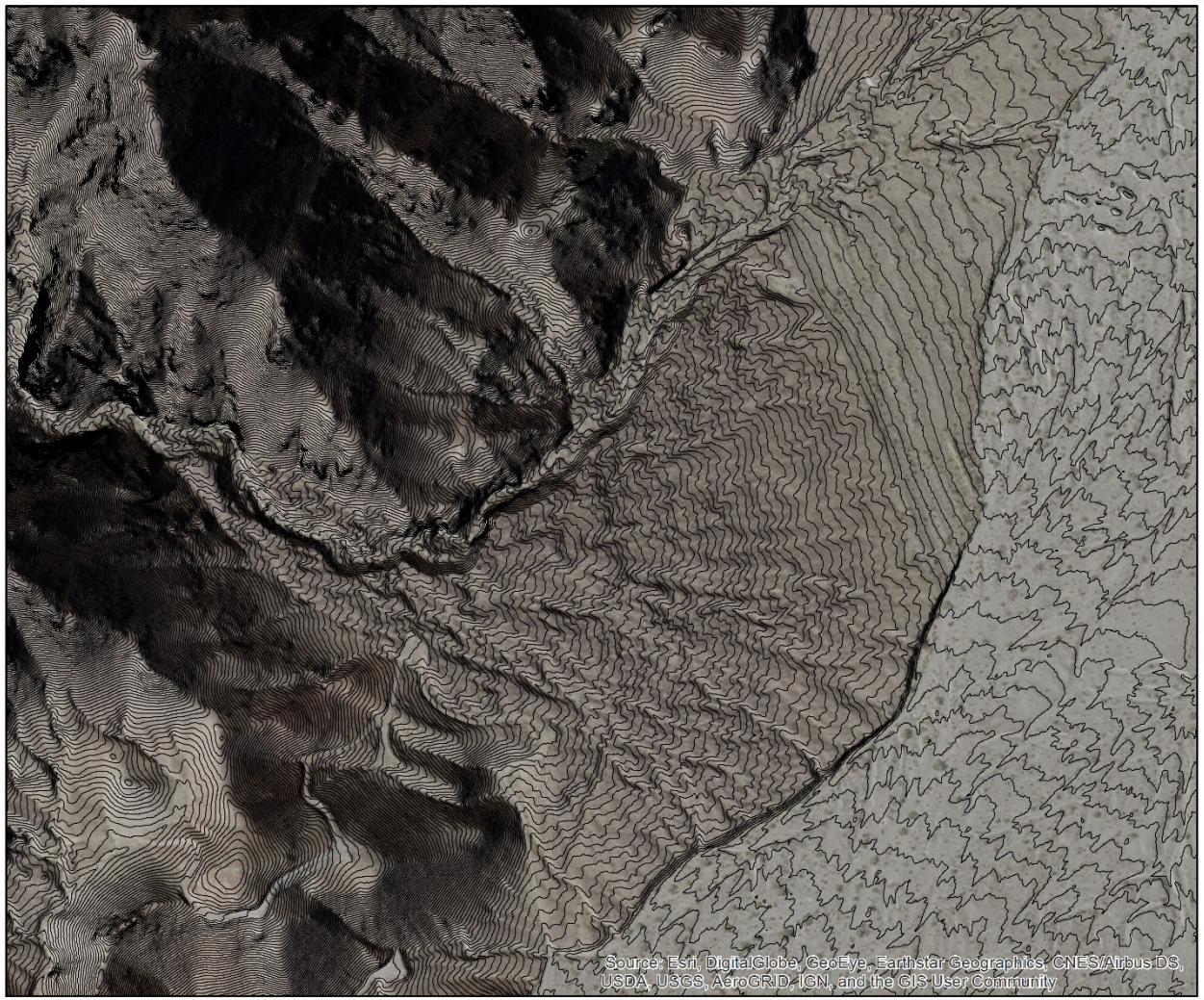

1:5,000

0 0.035 0.07 0.14 0.21 0.28 Kilometers

N

Figure 8.

In figure 10, profile A starts at a higher elevation at the feeder channel down to profile F located at a lower elevation. Profile D in the north end shows the active channel cuts through the fan and how much material has been buildup and spread out from the center of the fan. In profile E and F the fan width and buildup of material has decrease. Focusing on the profiles A – E from the north end. It shows the depth and width of the active channel. Examined more closely it shows that there where major flooding events that buildup levees on the edges of the active channel. This happens when floods overflow the channel and material is deposited on the sides of channels, profile D and E show that there were probably was one massive flooding event in the active channel or three events in the past. This is important information for mitigating potential floods hazards.

The topo map (figure 8) help discerner the Landsat image of figure 3, along with the analysis of the profiles, was used to create a detail Quaternary geological map (Figure 11). The Quaternary geological map units: Alluvial deposits (Qa), Alluvial Wash Deposits (Qw), Lacustrine, Playa, and Estuarine (Paralic) Deposits (Ql), Old Alluvial Valley Deposits (Qoa), Truckhaven Volcanics, Rhyolite and rhyolitic tuff (Ttv) and Quartz, diorite, light gray, massive to gneissoid, contains some xenoliths locally, abundant biotite, coherent (qd); were taken from the "alluvial fan task force" (AFTF) description and Thomas W. Dibblee (2008) from the same general area that had a scale of 1:750,000.

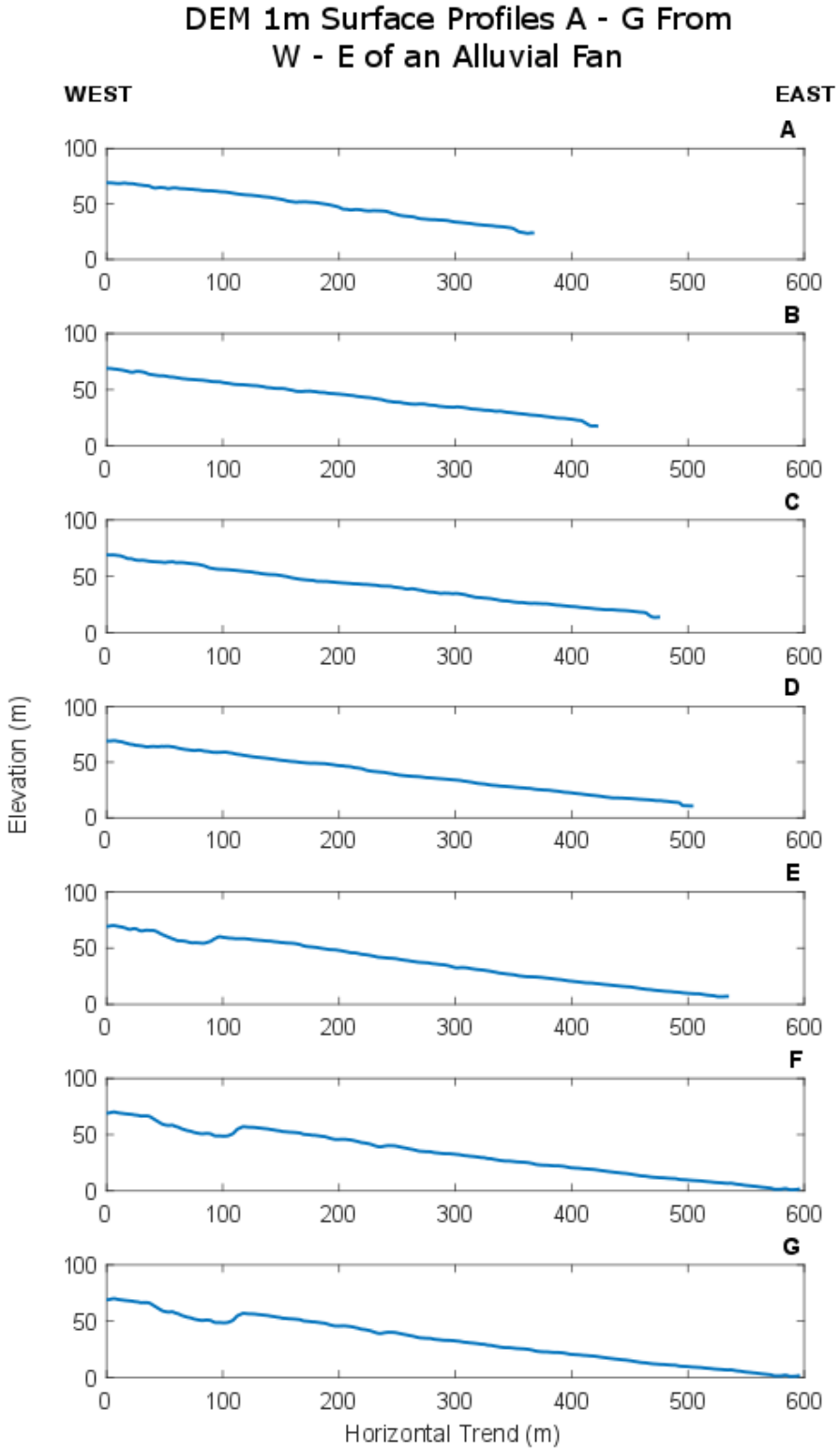

Figure 9. : Profiles A – G runs from the mouth of the alluvial fan towards the apex of the fan, where the trend of the profile runs west to east. The cross-sections of the alluvial fan shows the curvature of the fan whether the morphology is concave or convex.

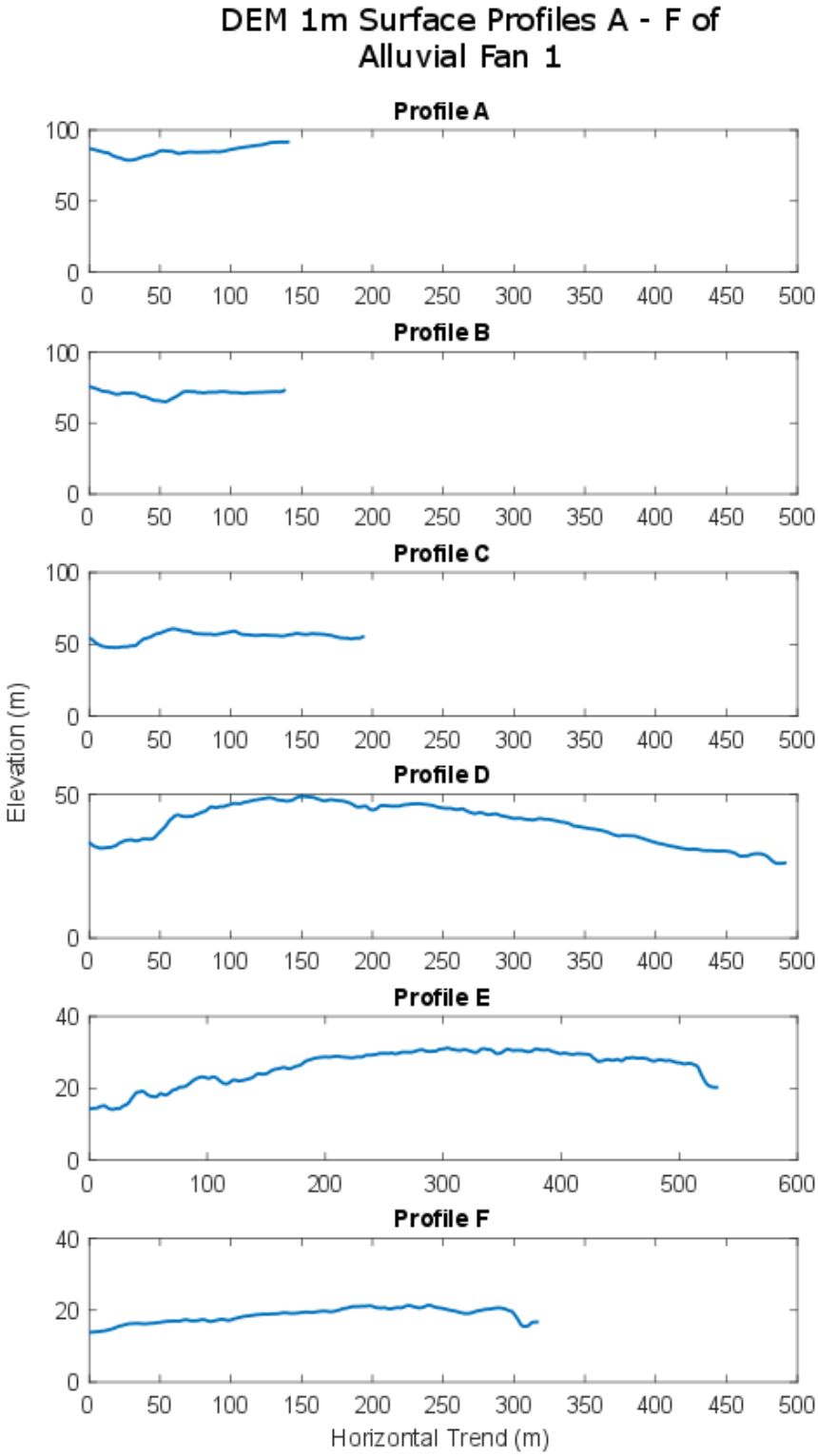

Figure 10. : Profiles A - F running horizontally from the mouth of the alluvial fan towards the Apex of the Fan, where the trend of the profile runs north to south.

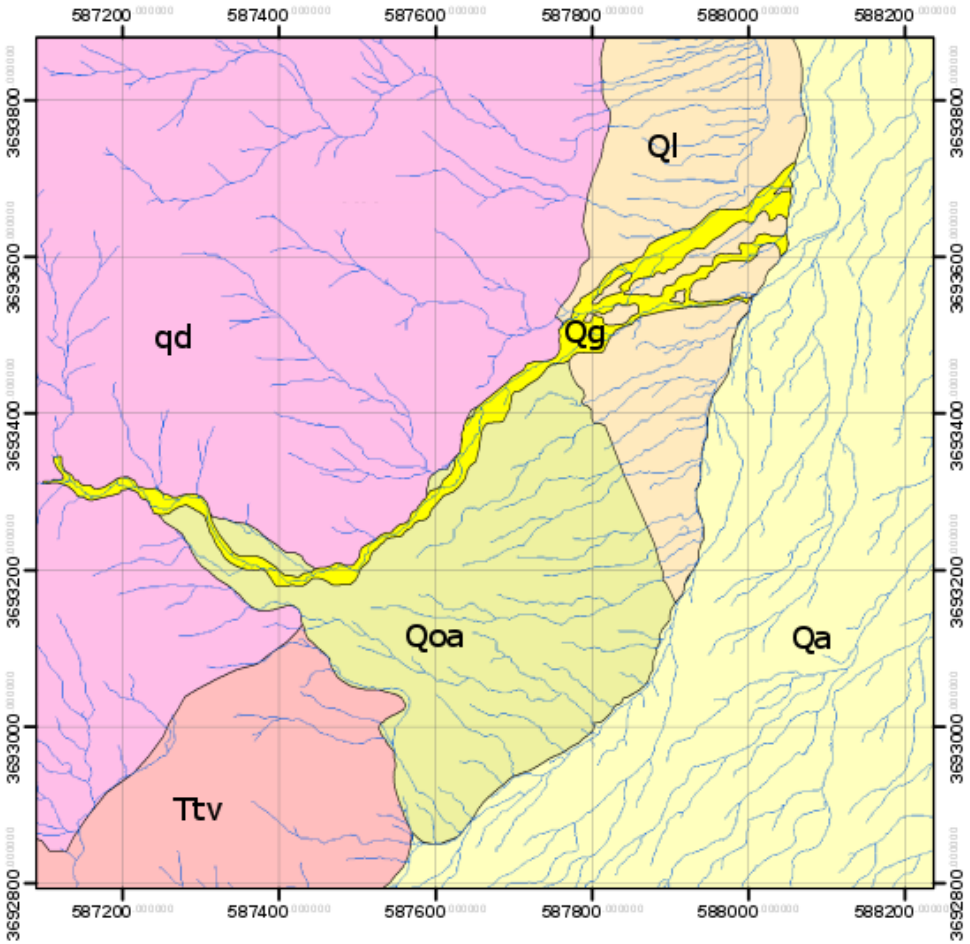

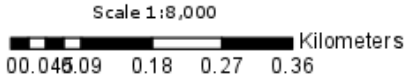

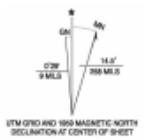

Figure 11.

GEOLOGICAL FEATURE MAP BASE ON THE CHARACTERISTICS OF THE 1-METER DEM

IMPERIAL COUNTY, CALIFORNIA

BY: ERIC A. MACLEOD

Qa	Unindurated, undissected alluvial Sediments; Age Holocene; Alluvial sand and sheet flow terrace deposits	Holocene	QUATERNARY	CENOZOIC
Qg	Unindurated, undissected alluvial Sediments; Age Holocene; Alluvial gravel and sand of stream washes	Holocene	QUATERNARY	CENOZOIC
Ql	Unindurated, undissected alluvial Sediments; Age Holocene; Lake deposits Sediments. Old shoreline of the Salton Sea.	Holocene	QUATERNARY	CENOZOIC
Qoa	Unindurated, undissected alluvial Sediments; Age Holocene; Alluvial sand, rocks, boulders and river terrace deposits	Pleistocene	QUATERNARY	CENOZOIC
Ttv	TRUCKHAVEN RHYOLITE; Age, ~Pliocene; Truckhaven Volcanics, rhyolite and rhyolitic tuff	Pliocene	TERTIARY	CENOZOIC
-- Unconformity --				
qd	PLUTONIC ROCK; Age, Paleozoic; Quartz Diorite, Light Gray, Massive to gneissoid, xenoliths, abundant biotite	CRETACEOUS	MESOZOIC	

Unit references: Thomas W. Dibblee (2008). Geological Map of the Clark Lake and Rabbit Peak 15 Minute Quadrangles, Riverside, San Diego, and Imperial Counties, California; Dibblee Geology Center Map #DF-374; https://ngmdb.usgs.gov/Prodesc/proddesc_83960.htm

Conclusion

The 1-meter DEM analysis of the alluvial fan showed alluvial fan morphology in detail. These results show that the 1-meter data is approximately the lowest spatial resolution data that can be used to map alluvial morphology. This is apparent in the lower spatial resolution (30m and 10m) DEM when looking at the alluvial fan. The contour patterns of each morphologic area provide a distinct signature or fingerprint for a given morphology (e.g. shore line, sheet flow, etc). A detailed geological map of Quaternary alluvium can be produced using (at least) 1-meter DEM data only. The appendix section demonstrates that DEMs using the Pearson's and Spearman's Ranked Correlation are similar. This means that the elevation does not influence the quality of the image, but it is the spatial data (density of information) that influence the quality of the image. Therefore, the higher spatial resolution of the 1-meter DEM has enough data to assist to interpret the terrains features to create a Quaternary geological map.

References

Arun P.V. "A comparative analysis of different DEM interpolation methods" The Egyptian Journal of Remote Sensing and Space Sciences (2013) 16, 133–139

Benrossian, T.L, Hayhurst, C.A. at el (2014) Surficial Geologic Mapping and Associated GIS Databases for Identification of Alluvial Fans; Environment and Engineering Geoscience, Vol XX No. 4, November 2014. Pp 335-348

Blair, T.C., McPherson, J.G., 2009. Processes and forms of alluvial fans. In: Parsons, A.J., Abrahams, A.D. (Eds.), Geomorphology of Desert Environments, second ed. Springer, Berlin, pp. 413–467.

Boggs, Sam (2006). Principles of Sedimentology and Stratigraphy, Pearson Prentice Hall NJ ISBN 0-13-154728-3

Bull, W.B., 1977. The alluvial fan environments. Geography 1, 222–270.

Chang, Kang-Tsung (2016). "Introduction to Geographic Information System", Eighth Edition, Mc Graw Hill Education

Christopher M. Bishop!, Markus Svense, Christopher K.I. Williams (1998); Developments of the generative topographic mapping, Elsevier Science B.V. 203–224

Chuanfa Chen , Yanyan Li & Tianxiang Yue (2013) Surface modeling of DEMs based on a sequential adjustment method, International Journal of Geographical Information Science, 27:7, 1272-1291, DOI: 10.1080/13658816.2012.704037

Dong Ren, Junqiao Zhang, Shuanghui Lei, Le Zhang; (2014). DEM Extraction Based On SFM Using Remote Sensing Images; College of Computer and Information Technology, China Three Gorges University

Dibblee, T.W., Jr., 1954, Geology of the Imperial Valley region, California, in Jahns, R.H., ed., Geology of Southern California: California Department of Natural Resources, Division of Mines Bulletin 170, p. 21–28.

Engel, A.E.J., and Schultejann, P.A., 1984, Late Mesozoic and Cenozoic history of south-central California: Tectonics, v. 3, no. 6, p. 659–675.

FEMA, 2003, Guidelines and specifications for flood hazard mapping partners; Appendix G: Federal Emergency Management Agency, Guidance for Alluvial Fan Flooding analyses and mapping.

Florsheim, J.L., 2004. Side-valley tributary fans in high-energy river floodplain environments: sediment sources and depositional processes, Navarro River basin, California. Geol. Soc. Am. Bull. 116, 923–937.

Gianluca Norinia, Maria Clara Zuluagab, Iris Jill Ortizc, d, Dakila T. Aquinoc, Alfredo Mahar F. Lagmayc, d; (2016) Delineation of alluvial fans from Digital Elevation Models with a GIS algorithm for the geomorphological mapping of the Earth and Mars; Geomorphology, Volume 273, 15 November 2016, Pages 134–149

Gibbon, J.D., 2011. Nonparametric Statistical Inference, fifth edition; Taylor and Francis Group ISBN: 978-1-4200-7761-2

Harvey, A.M., 2003. The response of dry-region alluvial fans to the late Quaternary climatic change. In: Alsharhan, A.S., Wood, W.W., Goudie, A.S., Fowler, A., Abdellatif, E.M. (Eds.), Desertification in the Third Millennium. Balkema, Rotterdam, pp. 83–98.

Harvey, A., Mather, A.E., Stokes, M., 2005. Alluvial fans: geomorphology, sedimentology, dynamics-introduction, a review of alluvial fan research. In: Harvey, A., Mather, A.E., Stokes, M. (Eds.), Alluvial fans: geomorphology, sedimentology, dynamics. Geological Society Special Publication 251, London, pp. 1–8.

Ingersoll, R.V. 2008. Reconstructing southern California, in Spencer, J.E., and Titley, S.R., eds., Ores and orogenesis: Circum-Pacific tectonic, geologic evolution, and ore deposits: Arizona Geological Society Digest 22, p.22 409-417.

Jenkins, David G., 2006. GIS, SINKS, FILL, and Disappearing Wetlands: Unintended Consequences in Algorithm Development and Use; University of Central Florida Department of Biology Orlando, FL, USA pg. 277-282

Lutz, A.T., 2006. Stratigraphic record of Pleistocene faulting and basin evolution in the Borrego Badlands, San Jacinto fault zone, Southern California; GSA Bulletin; November/December 2006; v. 118; no. 11/12; p. 1377–1397; doi: 10.1130/B25946.1

Manuel, P., 2004. Influence of DEM interpolation methods in drainage analysis. GIS Hydro 04. Texas, USA.

Mather, A.E., Harvey, A.M., Stokes, M., 2000. Quantifying long-term catchment changes of alluvial fan systems. Geol. Surv. Am. Bull. 112, 1825–1833.

Miller, J. Julianne (2011) Playa Lake Hazards and Resources. Flood Hazard Identification and Mitigation in Semi- and Arid Environments: pp. 109-131.

Minnie, Amanda., 2015. Perceptions of Namibian Primary School Teachers' and Stakeholders', in the Khomas Education Region, regarding curriculum requirements for sustaining a successful Physical Education program. University of Eastern Finland Philosophical Faculty, pg.50; http://epublications.uef.fi/pub/urn_nbn_fi_uef-20150986/urn_nbn_fi_uef-20150986.pdf

Mitas, L. and Mitasova, H. (1999). Spatial interpolation, in P. Longley, M.F. Goodchild, D.J. Maguire and D.W. Rhind (eds) Geographical Information Systems: Principles, Techniques, Management and Applications, Hoboken, NJ: John Wiley and Sons.

Mukherjeea Sandip., 2012. Evaluation of vertical accuracy of open source Digital Elevation Model (DEM); International Journal of Applied Earth Observation and Geoinformation 21 pg. 205–217

National Oceanic and Atmospheric Administration (NOAA), U.S. Department of Commerce; Data Access Viewer (DAV); URL: https://coast.noaa.gov/dataviewer/#/

NRC, 1996, Alluvial fan flooding: National Research Council, Committee on Alluvial Fan Flooding, Water Science and Technology Board, Commission on Geosciences, Environment, and Resources, National Academy Press, 172p.

Raymond T. Lenaburg (2010). Need for Updating Alluvial Fan Floodplain Delineation Guidelines: A White Paper; Risk Analysis Branch Mitigation Division, DHS-FEMA Region IX

Schick, A.P., Lekach, J., 1987. A high magnitude flood in the Sinai Desert. In: Myer, L., Nasch, O. (Eds.), Catastrophic Flooding. Allen and Unwin, Boston, pp. 381–409.

Stock J.D., Schimidt K.M., Miller D.M. (2008) Controls on alluvial fan long-profiles. Geological Society of America Bulletin

Thomas W. Dibblee (2008). Geological Map of the Clark Lake and Rabbit Peak 15 Minute Quadrangles, Riverside, San Diego, and Imperial Counties, California; Dibblee Geology Center Map #DF-374; https://ngmdb.usgs.gov/Prodesc/proddesc_83960.htm

Tian-Xiang Yue, Zhen-Ping Du, Dun-Jiang Song, Yun Gong (2007). "A new method of surface modeling and its application to DEM construction" Geomorphology 91 161–172

Trinda L. Bedrossian, Peter D. Roffers, and Cheryl A. Hayhurst; 2010. Geologic Compilation of Quaternary Surficial Deposits in Southern California; California Department of Conservation California Geological Survey

U.S. Geological Survey, 20160711, USGS NED 1 arc-second n34w117 1 x 1 degree IMG 2016 (a): U.S. Geological Survey.

U.S. Geological Survey , 20160711, USGS NED 1/3 arc-second n34w117 1 x 1 degree IMG 2016 (b): U.S. Geological Survey.

U.S. Geological Survey, 2010 Salton Sea Lidar Collection(Salton_Sea) services provided by the OpenTopography Facility with support from the National Science Foundation under NSF Award Numbers 1226353 & 1225810, https://doi.org/10.5069/G9V985ZF

Webb, R.H., Pringle, P.T., Rink, G.R., 1987. Debris flows from tributaries of the Colorado River, Grand Canyon National Park, Arizona. U.S. Geological Survey Open-File Report 1492, Washington, USA.

Winker, C.D., 1987, Neogene stratigraphy of the Fish Creek–Vallecito section, Southern California: Implications for early history of the northern Gulf of California and the Colorado Delta [Ph.D. thesis]: University of Arizona, 494 p.

Winker, C.D., and Kidwell, S.M., 1996, Stratigraphy of a marine rift basin: Neogene of the western Salton Trough, California, in Abbott, P.L., and Cooper, J.D.,eds., Field conference guidebook and volume for the American Association of Petroleum Geologists annual convention, p. 295–336.

Woodard, G.D., 1963, The Cenozoic succession of the west Colorado Desert, San Diego and Imperial Counties, Southern California [Ph.D. thesis]: Berkeley, University of California, 173 p.

Zheng Cui, Keqi Zhang at el. (2013), BigSpatial '13 Proceedings of the 2nd ACM SIGSPATIAL International Workshop on Analytics for Big Geospatial Data; ACM New York, NY, USA ISBN: 978-1-4503-2534-9 doi>10.1145/2534921.2534922

Zhao, B., & Mays, L. W. (1993). Uncertainty analysis of the FEMA method for alluvial fans. In H. W. Shen, S. T. Su, & F. Wen (Eds.), Proceedings - National Conference on Hydraulic Engineering (pt 2 ed., pp. 2098-2013). New York, NY, United States: Publ by ASCE.

Appendix A

A Mathematical Approach – variance of DEMs

Random Points

To quantify of how these DEMs may or may not correlate to one another. Random points were chosen using the 'create random points' function from the Data Management toolbox in ArcMAP, from the specified dimension from figure 3. Two large random sets of elevation numbers and their locations were produced. The distribution of points is seen in figure 12 and in table 1. A sample size of 1,000 random elevation points from two different sets were used for comparison to generate the figure. The observed correlation of the 1-meter DEM to the other two DEMs (10 and 30 meters), the sample size needs to be large enough to show that the size would show a very weak correlation can be significant (Gibbon, J.D., 2011). However, a small sample size might give false results because the area of figure 3 is large enough to give a very strong correlation that is not statistically significant, meaning that there is no relationship with the 1-meter DEM to the other DEMs would be a plausible explanation. That is why it is imperative to optimize the DEMs sample size with 1,000 random points would be appropriate to avoid false representation of the DEM images.

Two sets of 1000 Random points located at the Alluvial Fan

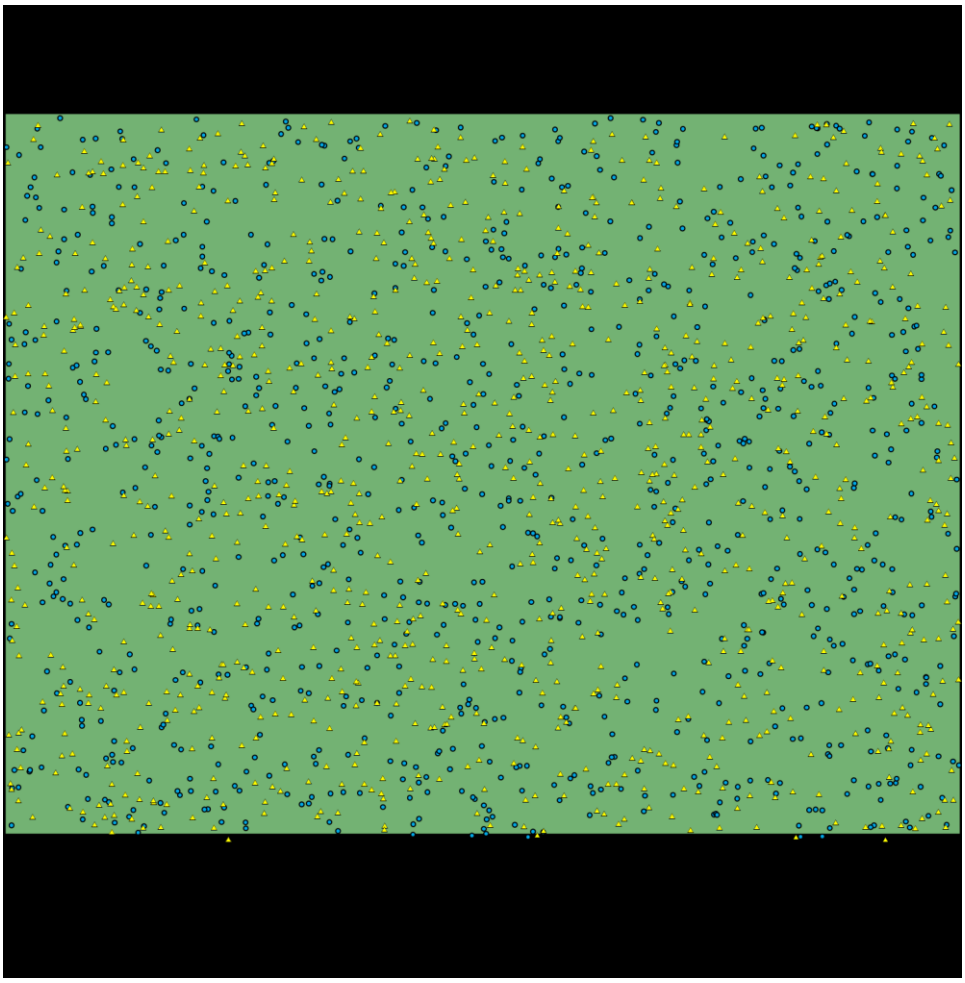

Figure 12: There are two sets of 1000 random points for the alluvial fan that is the focus of this study. Set 1 is in yellow and set 2 is blue. These random points (lat, lon) locations are used consistently for all of the DEMs to compare the similarities of elevation.

Spearman's Rank Correlation and Pearson Correlation of 1000 Random Numbers

DEM 1	DEM 30	Rank DEM 1	Rank DEM 30	d	d^2
209.098236	201.803864	1	8	-7	49
209.036835	210.120468	2	3	-1	1
208.028931	210.120468	3	3	0	0
206.666946	199.38945	4	12	-8	64
204.670517	199.38945	5	12	-7	49
203.964905	198.384552	6	15	-9	81
203.807907	203.554047	7	5	2	4
203.429489	201.848831	8	6	2	4
202.129608	216.525574	9	1	8	64
.	.	.	.	.	
.	.	.	.	.	
.	.	.	.	.	
-3.911116	-3.777423	996	993	3	9
-4.839572	-3.894406	997	996	1	1
-5.165989	-4.873704	998	999	-1	1
-5.185414	-4.873704	999	999	0	0
-5.389641	-3.894406	1000	996	4	16

Spearman's Rank Correlation
r = 1 6sumd^2 / n^3-n
sum of d^2
304561
Numerator
1827366
n
1000
n^3
1000000000
Denominator
999999000
r
0.998172632

Pearson Correlation DEM 1: DEM 30 -> 0.997424486

Table 1: There are 1000 random numbers that are in order from highest to lowest elevation value, comparing the 1-meter DEM to the 30-DEM using Spearman Rank Correlation and Pearson Correlation.

These random point attributes record the latitude and longitude as well as the elevation which is vital for the calculations. Figure 12 shows the two sets which were used and how the points are distributed in the area. Their locations (latitude and longitude) are used for all the DEMs to compare similarities in elevation data; a quantitative measurement on each set of random numbers will consider the 1-meter DEM setup against the 10-meter and 30-meter DEM to establish if there is a relationship between the two.

Spearmen's Rank and Pearson Correlation

Spearmen's rank correlation is a nonparametric statistical method to select random geographic points with their perspective elevations for this report. Spearman's correlation coefficient is represented by the symbol r or rho which measures the strength and direction of the 1-meter DEM that is being compared to another rank of variables i.e. 10-meter and 30-meter DEM. Spearmen's rank shows the monotonic relationship between the two DEM rather than the strength and direction of the linear relationship between the DEMs, which Pearson's correlation determines (Gibbon, J.D., 2011). Figure 13 shows three example of a monotonic relationship where the elevation of each DEM image increases or decreases retrospectivity with one another.

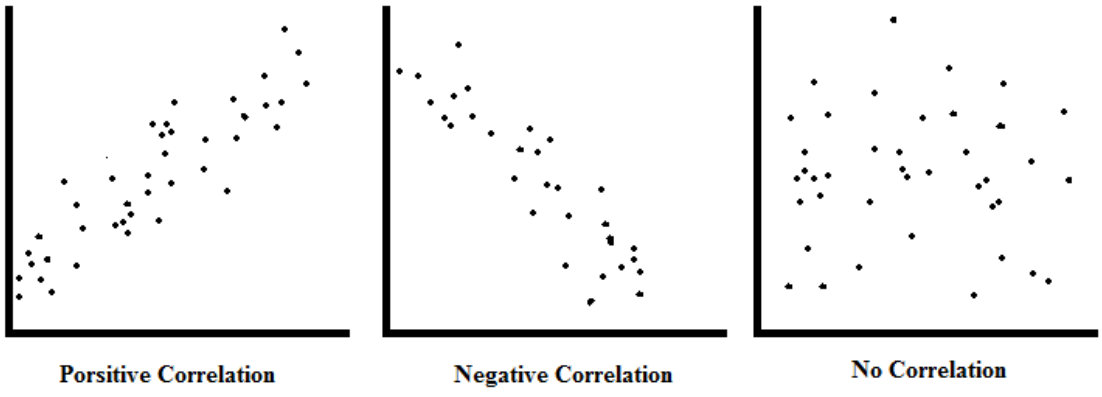

Figure 13. Shows graphs of how data can correlate

- Positive correlation – the elevation of the DEMs images has increase;
- Negative correlation – the elevation of the DEMs images has decrease;
- No correlation – the elevation of the DEMs images does not tend to either increase or decrease but looks like a bunch of random points

Table 1 categorizes the 1-meter DEM correlation by considering as one variable increases or decreases in elevation, to observe what happens to the other 10-meter and 30-meter DEMs. To make this observation; 1,000 random elevation points are matched with the 1-meter DEM and with the 10-DEM and the 30-meter DEM. There are two sets of random points that correspond to the three DEMs which means there are a total of six different random elevation points that relate to the DEMs. Since the random points have the same latitude and longitude in each set, the location does not need to be considered. The random elevation points are matched to each DEM shown in figure 13, using ArcGIS. A linear regression can be formulated between the 1-meter DEM and the 10-meter and 30-meter DEMs. Figure 14 shows the relationship between the elevation from the 1-meter DEM and the corresponding altitude of 10-meter and 30-meter; denotes that there is a positive correlation with the DEMs.

To further identify and test the strength the relationship has between the DEMs we need to show a statistical method that will either prove or disprove how similar the DEM images by calculating the rho value. This will provide a percentage of how close the DEM images relate to each other. The statistical measurement of the DEMs (figure 16), when graph shows that the strength of the linear relationship between the paired DEM data does have a positive correlation. So, the assumption is that the r value would show the same

direction (positive). The linear regression shows the DEMs are closely related but not how strongly the DEMs related to one another. Spearmen's rank correlation is used to generate the general formula for calculating how strong the DEMs correlate, which is seen below:

$$\rho = 1 - \frac{6\sum d_i^2}{n(n^2-1)}$$

https://statistics.laerd.com/statistical-guides/spearmans-rank-order-correlation-statistical-guide.php

Where:

d = is the difference between the two DEMs of each observation that correlates to the elevation.

n = number of observations which is 1,000

Rho or **r** = shows the correlation of the DEMs

To describe the strength of the correlated value of rho is given below:

- .00-.19 "very weak"
- .20-.39 "weak"
- .40-.59 "moderate"
- .60-.79 "strong"
- .80-1.0 "very strong" (Minnie, 2015)

The correlation of the DEMs which is denoted by r can only be negative or positive that is constrained by design as:

$$-1 \leq r \leq 1$$ (Minnie, 2015)

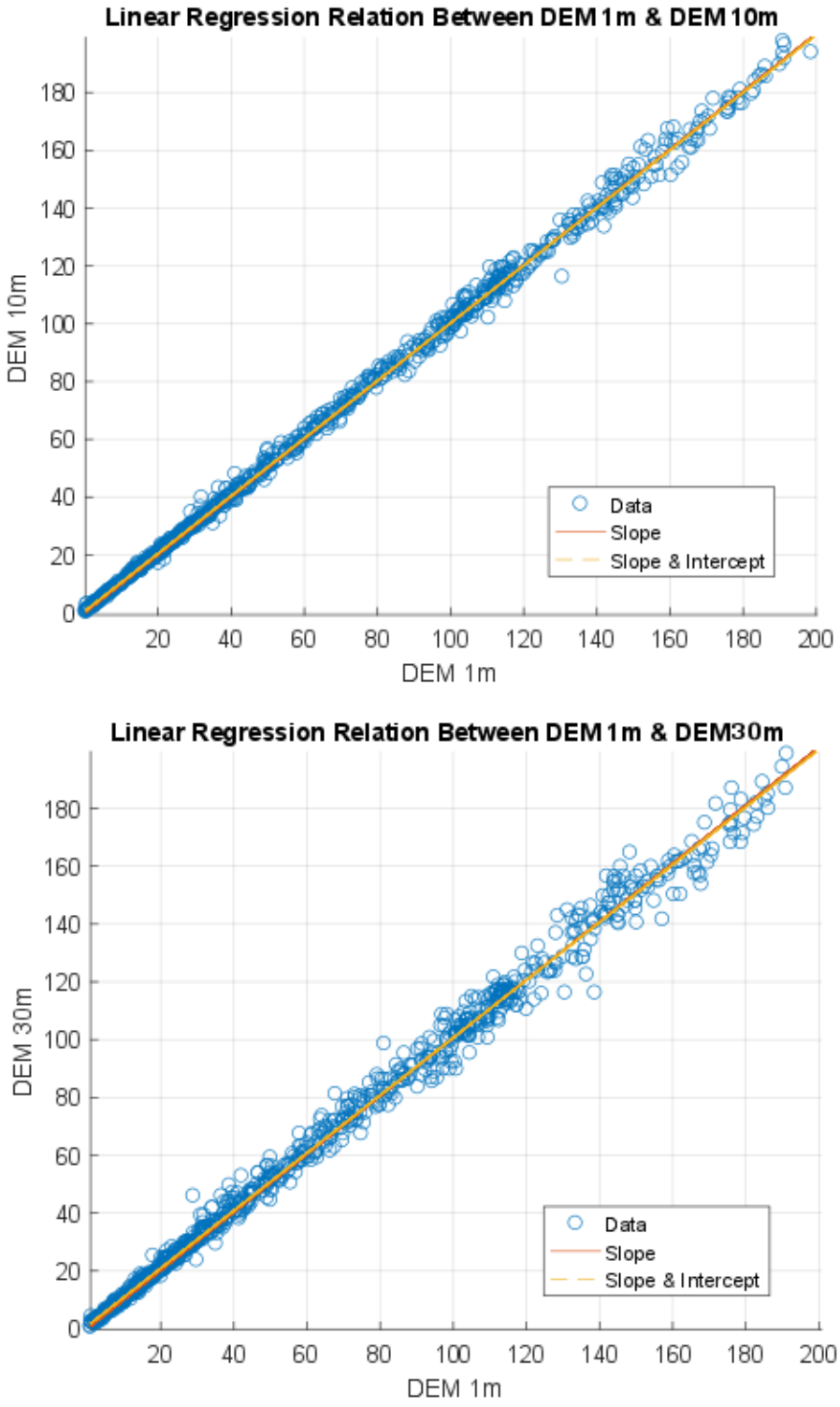

Figure 14.
Positive values denote positive linear correlation

The linear regression of figure 14 is positive so the relationship of the elevation can only be positive. As you look at the result in table 1, the rho value is 0.998 which means it is very strongly correlated to its constrained value of 1 (Minnie, 2015). This indicates that there is no difference in the DEMs. Since the DEMs have been proven to be similar it would be astute to check the results with another method to test the strength and direction of the linear relationship between the DEMs, using Pearson's correlation (Gibbon, J.D., 2011). The formula is as follows:

$$r_{xy} = \frac{\sum x_i y_i - n\bar{x}\bar{y}}{n s_x s_y} = \frac{n\sum x_i y_i - \sum x_i \sum y_i}{\sqrt{n\sum x_i^2 - (\sum x_i)^2}\,\sqrt{n\sum y_i^2 - (\sum y_i)^2}}.$$

Eq taken from Wiki: https://en.wikipedia.org/wiki/Correlation_and_dependence

Where,

x = Elevation values in 1-meter DEM

y = Elevation values that are being compared to **x** i.e. 10-meter and then 30-meter DEM

n = Total number of values which is 1,000.

Rho or **r** = Pearson correlation coefficient

These approaches calculate the relationships and tests the strength and direction the DEMs have towards one another. Once again in table 1 it shows that the Pearson correlation

coefficient rho is 0.997, the difference of the two methods is 0.001, meaning that the DEMs are the similar.

Spearman's Rank DEM Correction values

Comparing the first random set:

1-meter DEM to the 10-meter DEM, the r value is 0.9935

1-meter DEM to the 30-meter DEM, the r value is 0.9981

Comparing the second random set:

1-meter DEM to the 10-meter DEM, the r value is 0.9999

1-meter DEM to the 10-meter DEM, the r value is 0.9980

By normal standards, the association between the two variables would be considered statistically significant. However, since the values are close to positive 1 and Spearman > Pearson by a difference of 0.001, that means that the correlation is monotonic and linear because the difference of the two methods are too small to be significant. A further analysis of this can be seen in appendix B

Appendix B

How does spatial resolution impact elevation?

It was determined that Spearmen's Rank Correlation and Pearson Correlation are nearly 100% similar when comparing the two sets of random elevation points taken from the DEM's. It means that there is not enough difference between the elevations when comparing the higher 1-meter DEM resolution to the 10-meter DEM and 30-meter DEM. To further investigate this manner and make the accusation more robust, a more quantitative surface characterization is going to have to be used. The new parameters are going to be selected base on the Quaternary geological map (figure 11) that was produce using the 1-meter DEM topographic map (figure 8). This should allow a clear dissemination of the different types of morphologies and DEM's elevations correlation.

The obvious parameters for recalculating Pearson Correlation and Spearmen's Rank Correlation is going to be based on the Quaternary geological map (figure 11), categorizing the parameters into three main morphologies:

1) Flood Plan Zone

2) Alluvial Fan Zone

3) Mountainous Zone

Using the same random elevation points from figure 12 and using the three-morphological features to create three polygons in ArcMap. This will either further amplify the original results in appendix A or show that the DEM's elevation is affected by different morphologies. The three geological features are shown in figure 15 and how the two sets

of random points are distributed. Table 2 shows the two set of random points only forcing on the alluvial fan. Once again, the Pearson and Spearmen's Rank Correlation shows that the DEMs are similar. Therefore, the geological features do not impose any influence on the quality of the images.

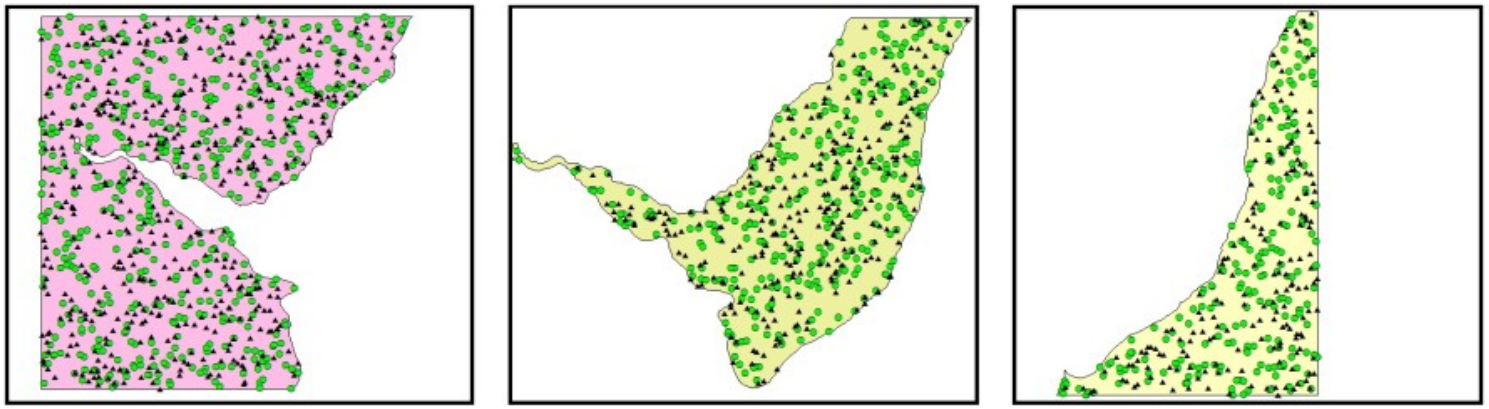

Figure 15. The green dots are the first set of random numbers and the black triangles are the second set of random numbers. The amount of green dots and black triangle retrospectivity (a) 382 pts and 515 (b) 307 pts and 298 pts;(c) 211 pts and 187 pts

Spearman's Rank Correlation and Pearson Correlation on the Alluvial Fan

DEM 1m	DEM 10m	DEM 30m							
FAN set1	FAN set11	FAN set111	Rank DEM 1	Rank DEM 10	d	d^2	Rank DEM 30	d	d^2
113.304008	115.88826	116.191391	1	1	0	0	2	-1	1
112.480629	113.791534	118.681763	2	2	0	0	1	1	1
96.37796	100.759628	95.255905	3	3	0	0	3	0	0
94.732651	96.513382	95.255905	4	4	0	0	3	1	1
94.000198	92.471634	93.709885	5	7	-2	4	5	0	0
93.601196	92.471634	93.709885	6	7	-1	1	5	1	1
93.586067	94.982071	93.709885	7	5	2	4	5	2	4
92.828125	94.023376	93.709885	8	6	2	4	5	3	9
.	.	.	.	.	.	.	.	.	.
.	.	.	.	.	.	.	.	.	.
.	.	.	.	.	.	.	.	.	.
-1.959747	-0.811119	-0.711361	304	301	3	9	302	2	4
-2.099687	-1.470779	-0.841092	305	303	2	4	303	2	4
-2.134856	-2.067909	-2.529555	306	306	0	0	304	2	4
-3.373115	-3.029266	-4.138739	307	307	0	0	307	0	0

Spearman's Rank Correlation	Spearman's Rank Correlation
FOR DEM 1 to 10	FOR DEM 1 to 30
r = 1 6sumd^2 / n^3-n	r = 1 6sumd^2 / n^3-n
sum of d^2	sum of d^2
5006	13252
Numerator	Numerator
30036	79512

n	n
307	307
n^3	n^3
28934443	28934443
Denominator	Denominator
28934136	28934136
z	r
0.998961918	0.997251966

Spearman Rank Correction	*DEM1m FAN set1*	*DEM 10m FAN set11*
FAN set1	1	
FAN set11	0.999061654	1
	DEM 1m FAN set1	DEM 30m FAN set111
FAN set1	1	
FAN set111	0.997850841	1

Table 2.